

## FULL PAPER

Discovery of *N*-pyridoyl- $\Delta^2$ -pyrazolines as Hsp90 inhibitorsSundeep Kadasi<sup>1,2</sup> | Ravali Yerroju<sup>1</sup> | Swetha Gaddam<sup>1</sup> | Nikhila Pullanagiri<sup>1</sup> |  
Meghana Chary<sup>1</sup> | Divya Pingili<sup>3</sup> | Shiva Raj<sup>2</sup> | Nulgumnalli Manjunathaiah Raghavendra<sup>1,4</sup> <sup>1</sup>Department of Pharmaceutical Chemistry, Gokaraju Rangaraju College of Pharmacy, Osmania University, Hyderabad, India<sup>2</sup>Department of Chemistry, Osmania University, Hyderabad, India<sup>3</sup>Sri Venkateshwara College of Pharmacy, Osmania University, Hyderabad, India<sup>4</sup>Department of Pharmaceutical Chemistry, Acharya & BM Reddy College of Pharmacy, Bengaluru, India

## Correspondence

Nulgumnalli M. Raghavendra, Department of Pharmaceutical Chemistry, Acharya &amp; BM Reddy College of Pharmacy, Acharya Dr. Sarvepalli Radhakrishnan Road, Soladevanahalli, Chikkabanavara Post, Bengaluru, Karnataka 560107, India. Email: nmraghava@yahoo.in

## Funding information

Department of Health Research, Grant/Award Number: V.25011/283/2014-HRV.; Rajiv Gandhi University of Health Sciences, Grant/Award Number: Advanced Research Project 2019-2020

## Abstract

Hsp90, as a key molecular chaperone, plays an important role in modulating the activity of many cell signaling proteins and is an attractive target for anticancer therapeutics. Herein, we report the discovery of *N*-pyridoyl- $\Delta^2$ -pyrazoline analogs as novel Hsp90 inhibitors by integrated approaches of drug design, organic synthesis, cell biology, and qualitative proteomic analysis. Novel chemical compounds were designed and optimized in the adenosine triphosphate-binding site of Hsp90; lead optimized compounds were found to have significant interactions with Asp93 and other amino acids crucial for Hsp90 inhibition. The designed compounds were synthesized by a two-step procedure; different aromatic aldehydes were reacted with various acetophenones to form substituted 1,3-diphenyl-prop-2-enones (**1c-1o**), which upon reaction with isonicotinic acid hydrazide in the presence of glacial acetic acid form *N*-pyridoyl- $\Delta^2$ -pyrazoline compounds (**PY1-PY13**). Compounds **PY3**, **PY2**, and **PY1** were identified as potential leads amongst the series, with promising anticancer activity against human breast cancer and melanoma cells, and the ability to inhibit Hsp90 similar to radicicol by drug-affinity responsive target stability proteomic analysis in a whole-cell assay.

## KEYWORDS

anticancer activity, inhibitors, pyrazole, rational drug design

## 1 | INTRODUCTION

Hsp90 (heat shock protein 90) is a prevalent protein in mammalian cells. Hsp90 functions as a molecular chaperone in the conformational maturation, stability, and trafficking of several client proteins into their biologically active forms.<sup>[1]</sup> Many Hsp90 client proteins are over-expressed in cancer and are responsible for unrestricted cancer cell proliferation and survival.<sup>[2]</sup> Prominent oncoproteins that are stabilized and assisted by Hsp90 for oncogenesis are BRAF, Akt, Her2, cdk4, Src, Flt-3, hTert, c-Met, Bcr-Abl, and so forth.<sup>[3,4]</sup> Inhibition of Hsp90 results in the simultaneous destabilization and degradation of multiple oncogenic client proteins, leading to cancer cell growth inhibition and apoptosis.<sup>[5]</sup> The pharmacologic blockade of the Hsp90 function is claimed to have a combined inhibitory activity on all the hallmark traits

of malignancy.<sup>[6]</sup> In addition, Hsp90 has been identified as an important extracellular mediator for tumor invasion,<sup>[7]</sup> and the expression of Hsp90 is also found to be amplified in cancer cells than normal cells.<sup>[8]</sup> Thus, the discovery of Hsp90 inhibitors is considered an important endeavor for anticancer drug development.

The complex natural product geldanamycin (GA) obtained from *Streptomyces hygroscopicus* was the first natural Hsp90 inhibitor reported.<sup>[9]</sup> Although too toxic to be developed as an anticancer drug,<sup>[10]</sup> its optimization by semisynthesis resulted in two promising derivatives: 17-allylamino-17-demethoxygeldanamycin (17-AAG) and 17-(2-dimethylamino)ethylamino-17-demethoxygeldanamycin (17-DMAG), which are more bioavailable than geldanamycin.<sup>[11,12]</sup> The concern regarding the toxicity of geldanamycin analogs due to their redox-active quinone moiety<sup>[12,13]</sup> led to the discovery of similar pharmacophoric compounds, such as mabecins<sup>[14]</sup> and herbimycins<sup>[15]</sup> with potent anticancer activity, which are presently under clinical trial. Radicicol (RAD), an antibiotic obtained from *Chaetomium chiversii*, is the

**Abbreviations:** DARTS, drug-affinity responsive target selectivity; Hsp90, heat shock protein 90; GA, geldanamycin; RAD, radicicol.

most potent inhibitor of Hsp90 *in vitro*, but the reactivity of its epoxide group and the sensitivity of its conjugated double bonds to Michael additions render it inactive *in vivo*.<sup>[16]</sup> Gedunin, a tetranortriterpenoid isolated from the Indian neem tree (*Azadirachta indica*), which was reported to have anticancer, antimalarial, and anti-inflammatory properties, is under clinical investigation.<sup>[17,18]</sup>

Experience with natural products generated interest in alternative chemotypes. The purine class of compounds were the first synthetic compounds discovered to have potent Hsp90 inhibition.<sup>[19]</sup> Using high-throughput screening, a novel 3,4-diaryl pyrazole resorcinol (CCT018159) was identified to have potent Hsp90 inhibition.<sup>[20]</sup> NVP-AUY922 (VER52296) is an isoxazole derivative initially developed by optimization of a lead compound (CCT018159) and exhibits strong anticancer activity against many mammalian cancer cells.<sup>[21]</sup> Computational approaches have produced many types of small-molecule Hsp90 inhibitors, including pyrazoles,<sup>[22]</sup> resorcinol-containing triazoles,<sup>[23]</sup> isoindoles,<sup>[24]</sup> imidazoles,<sup>[25]</sup> indazol-4-ones,<sup>[26]</sup> and so forth. The focused approach on the discovery of Hsp90 inhibitors credited with many compounds in clinical trials such as NVP-AUY922 (phase II; Novartis),<sup>[27]</sup> ganetispib (STA-9090, phase II; Synta),<sup>[28]</sup> XL-888 (phase I; Exelixis),<sup>[29]</sup> PU-H71 (phase I; Memorial Sloan-Kettering Cancer Center),<sup>[30]</sup> PF-4929113/SNX-5422 (phase I; Pfizer),<sup>[31]</sup> and so forth (Figure 1). Though adenosine triphosphate (ATP)-binding site ligands are

diverse in their chemical structure, they often bind to multiple proteins due to their nonspecificity. Nonselective ATP-binding ligands interact with many proteins, exhibiting toxicity and leading to the failure of a drug.<sup>[32,33]</sup> The N-terminal domain of Hsp90 is homologous to the members of the Hsp90 family, as well as to the members of the ATPase/kinase GHKL superfamily.<sup>[34]</sup> Molecular design and optimization of a selective N-terminal domain Hsp90 inhibitor is a challenging and complex process. Integrated approaches of bioinformatics, medicinal chemistry, and polypharmacology are to be given importance in developing Hsp90 inhibitors.

In continuation of our quest toward the discovery of small-molecule inhibitors of Hsp90,<sup>[35-38]</sup> in this article, we report the molecular modeling, chemical synthesis, and biological evaluation of *N*-pyridoyl- $\Delta^2$ -pyrazolines as Hsp90 inhibitors.

## 2 | RESULTS AND DISCUSSION

### 2.1 | Molecular modeling and docking simulations

We began our study by formulating a hypothesis to simulate constraints that approximate better interactions in the ATP-binding site of Hsp90. The initial approach treats this binding site as rigid

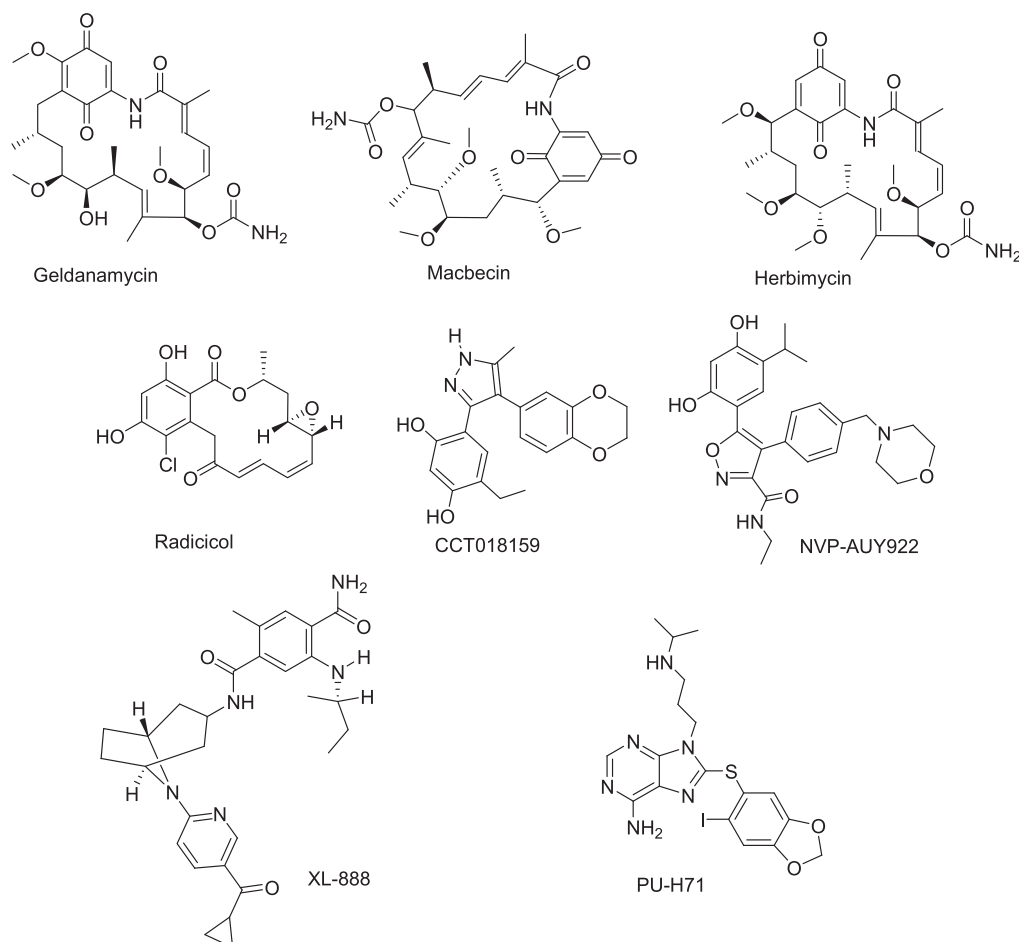


**FIGURE 1** Representative example of potential Hsp90 inhibitors of both natural and synthetic origin

while probing the conformational freedom of test ligands to establish a complementary shape in the active site. Pyrazole scaffold inhibitors of Hsp90 and insights gathered from the study of the ATP-binding site of Hsp90 motivated the selection of a trisubstituted pyrazoline scaffold for targeting Hsp90 protein.<sup>[22,25,39,40]</sup> Active site prediction by DoGSiteScorer reveals the ATP-binding site as the best binding pocket for Hsp90 protein (Table S1).<sup>[42]</sup> The validation of docking methodology through the “pose selection” approach by superimposing the crystal ligand and the redocked ligand of Hsp90 protein shows similar binding interactions, binding alignments, and satisfactory RMSD between superimposed crystal ligand and redocked ligand (Table S2).<sup>[42]</sup> Schrodinger’s Glide XP docking<sup>[43]</sup> of pyrazoline analogs in the rigid binding site of Hsp90 (PDB ID: 1YET)<sup>[44]</sup> endorse PY series having significant binding interactions with Hsp90 protein (Figure 2a–d). The detailed docking interactions are given in Table S3. The structure–activity relationship of the lead molecules of PY series was explored considering the binding interactions and their orientations in the ATP-binding site of Hsp90, with natural Hsp90 inhibitor GA and synthetic heterocyclic ligand “NVP-AUY922” (Luminespib) protein complexes. The N-terminal ATP-binding site of the Hsp90–GA complex indicates that it is a 15 Å deep cone/pyramidal shape pocket, 12 Å in diameter at the top surface and 8 Å wide midway of the pocket.<sup>[44]</sup> The nature of the binding site is described

as a combination of polar and hydrophobic natures imparted by 17 amino acids lining the interior of the pocket, with increasing hydrophobicity down to the bottom of the pocket, except induced polarity (negative electrostatic potential) due to the amino acid Asp93 and a polar residue Thr184, which are found to be crucial for making ligand–protein polar-bonding interactions. The surface of the binding site is mostly polar (positive electrostatic potential) with polar residues, Lys 58 and Lys 112, important for making polar interactions with the ligand. The pyridyl moiety of PY3 is directed toward the adenine-binding pocket of the natural substrate ADP at the bottom of the site, making crucial H-bonding interactions with amino acids Asp93 and Ser52 (Figure 2).<sup>[45]</sup> A similar interaction was found with the carbamate residue of GA with Asp93, which is likely to be a crucial interaction amongst the Hsp90 inhibitors. In addition, the pyridyl “NH” of PY3 makes another important polar interaction with Ser52, which was observed with the OH-resorciny moiety of NVP-AUY922 and the carbamate of GA, suggesting that Asp93 and Ser 52 are important residues for protein–ligand interactions.<sup>[21]</sup> A polar ‘NH’ of the heterocyclic ring is an essential pharmacophoric feature for ligand binding in the design of Hsp90 inhibitors. The central pyrazoline ring of PY3 overlaps the ribose sugar pocket of bound ADP and the 5-phenyl ring of PY3 is oriented toward Phe138, creating hydrophobic stacking interactions. The 4'-OH group of the

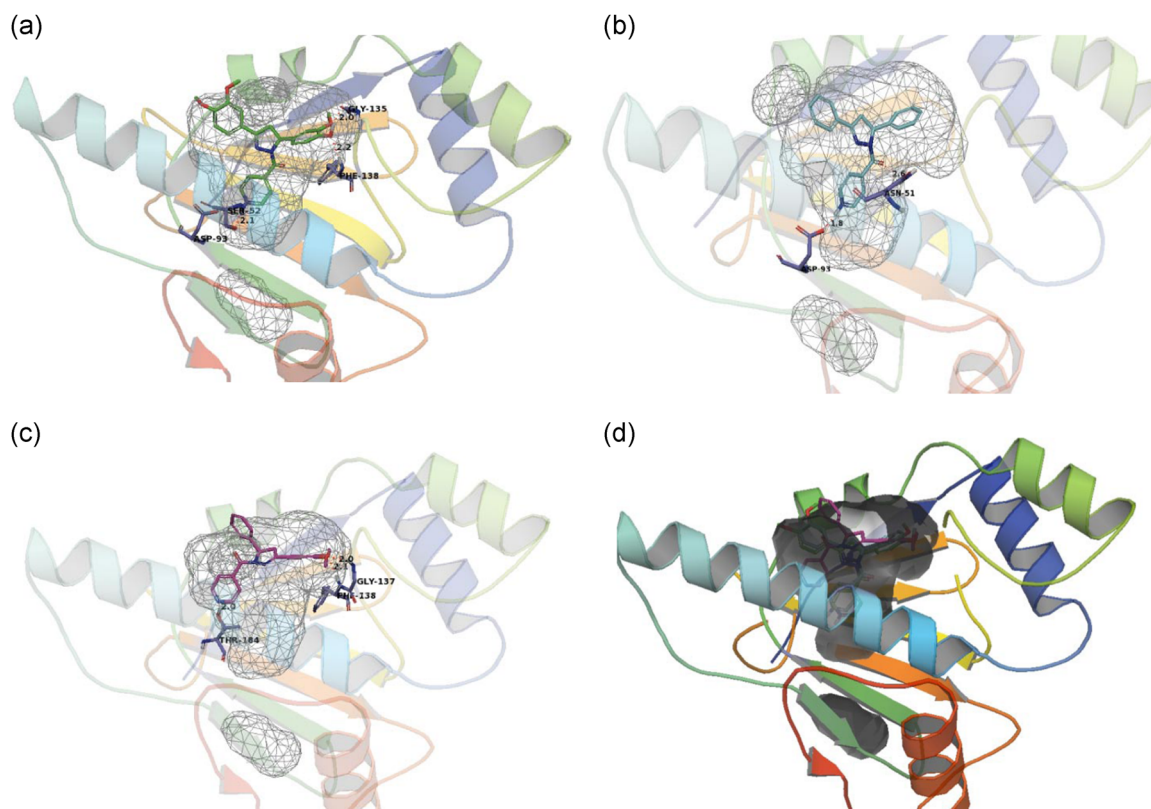


**FIGURE 2** Binding interactions of PY1–PY3 in the adenosine triphosphate-binding site (mesh or surface representation) of Hsp90 protein (cartoon shape; PDB ID: 1YET). (a) H-bonding interactions of green-colored stick form PY3 with blue colored stick forms of Asp 93 (2.1 Å), Ser 52 (2.1 Å), Phe 138 (2.2 Å), and Gly 135 (2.0 Å). (b) H-bonding interactions of cyano colored stick form PY1 with Asp 93 (1.8 Å) and Asn 51 (2.6 Å). (c) H-bonding interactions of purple-colored stick form PY2 with Thr 184 (2.0 Å), Phe 138 (2.1 Å) and Gly 137 (2.0 Å). (d) Overlap of stick forms of PY3 (green color), PY1 (cyano color), and PY2 (purple color) in the active site of Hsp90 protein (cartoon shape; PDB code 1YET)

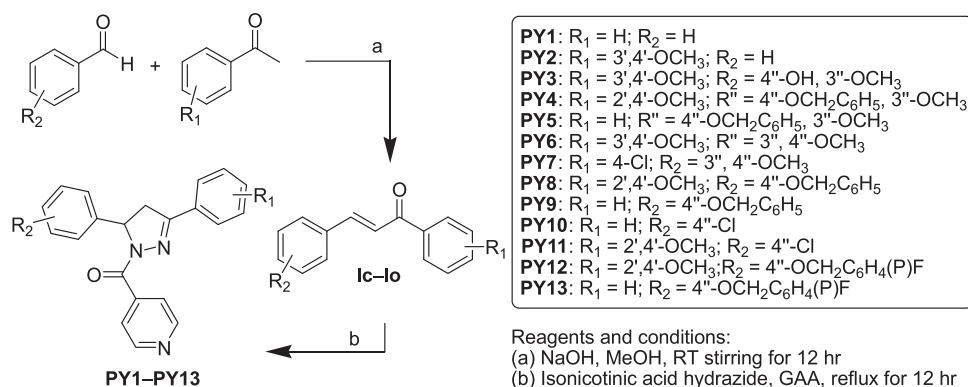
phenyl ring makes another H-bonding interaction with Gly135, stabilizing the complex, which is found in proximity to the planar amide group of GA. Ligand **PY1** showed hydrogen bonding interactions with Asp93 and Asn51; the latter is in proximity to the Ser52, making important H-bonding interactions. Ligand **PY3** shows a polar H-bonding interaction with Thr184, similar to carbamate of GA, establishing that Asp93, Thr 184, Ser52 are very crucial for protein binding. Ligand **PY2** interacts with Thr184 and a stabilizing interaction with amino acids Gly137 and Phe 138. Ligand **PY4** shows a slightly different orientation in the ADP-binding site, without any significant interaction with Asp93, Ser52, or Thr184, due to bulkiness in its molecular structure and slightly greater rotational penalty (0.3), yet making important hydrophobic interactions with amino acids Val150, Leu107, Val136, Val186, Ala55, Met98, and ranks below the lead molecules. **PY5** interacts with Asp93 with an H-bond parameter of  $-0.9$  and hydrophobic interactions with amino acids Ala55, Phe138, Gly135, Val136, Leu107, suggesting it to be moderately binding in the active site. **PY6** interacts in a similar way with Asp93, but the molecule is slightly low on the polar H-bond parameter ( $-0.6$ ), suggesting it is a weakly binding ligand in docking analysis and cytotoxicity study. Although ligand **PY7** found to have a hydrogen bond with Asp93, it has low electrostatic interactions and therefore has low binding affinity than **PY1**, **PY2**, and **PY3**. **PY8**, **PY9**, **PY10**, **PY11**, and **PY13** do not show any significant interaction with a crucial amino acid Asp93 and hence, are placed down the table in terms of binding affinity, which corroborates with the cytotoxicity assay. Although **PY12** has significant interaction with Asp93, it is ranked low in the cytotoxicity assay and docking analysis as the molecule possesses greater rotational flexibility and a greater number of binding poses with a greater scope for nonselectivity.

The SAR analysis of pyrazolines alludes to the importance of a trisubstituted pyrazoline scaffold with a heterocyclic "NH" oriented toward the bottom of the binding pocket (adenine-binding site of ADP) as an important pharmacophore. The presence of polar OH/OCH<sub>3</sub> at the 3',4'/3'',4''-positions of the benzene ring contribute toward stabilizing interactions of protein-ligand complex, increasing the polar and electrostatic parameters for the drug-like molecules, whereas electro-negative atoms do not alter any binding affinity. Aromatic rings at the 3,5-position of the pyrazoline and the heterocyclic aromatic ring at the

1-position of pyrazoline are crucial for nonpolar interactions with hydrophobic residues of the protein. Heterocyclic pyrazoline is essential for projecting the pharmacophoric features for essential interactions with vital amino acids. To further evaluate the polar interactions in the ATP-binding site of Hsp90, docking simulations were performed with different crystal complexes of Hsp90 protein available in the protein data bank (PDB:ID 2BYH, 1OSF, and 4EGK).<sup>[39,46,47]</sup> Polar interactions of the PY series are given in Table S4.

## 2.2 | CHEMISTRY

The synthetic protocol of *N*-pyridoyl- $\Delta^2$ -pyrazolines (depicted in Scheme 1) began with a Claisen-Schmidt reaction between various substituted benzaldehydes and substituted acetophenones to form 1,3-diphenyl-prop-2-enone derivatives (**Ic-Io**). Purification of 1,3-diphenyl-prop-2-enones was done by flash chromatography in the yields 72–85%. Subsequently, the nucleophilic addition reaction of isonicotinic acid hydrazide with the individual 1,3-diphenyl-prop-2-enones in glacial acetic acid (as solvent), yielded cyclized pyrazolines (**PY1-PY13**) in 25–35%. The structures of the final *N*-pyridoyl- $\Delta^2$ -pyrazoline compounds (**PY1-PY13**) were confirmed by <sup>1</sup>H-NMR studies, and all the compounds were found to have three characteristic peaks of a doublet of doublets (dd) around 3.2–3.3, 3.7–3.8, and 5.6–5.8 ppm (parts per million), due to *J*<sub>abx</sub> coupling of protons on the pyrazoline ring. The infrared (IR) and mass spectral data also confirmed the structural details of *N*-pyridoyl- $\Delta^2$ -pyrazoline compounds (**PY1-PY13**). A single crystal of **PY1** was obtained by recrystallization from chloroform at room temperature (22 to 24°C). X-ray diffraction of **PY1** was measured using radiation of wavelength 0.71073 Å at 296 K (Figure 3). The crystal system and space group were found to be monoclinic and P2(1)/c (detailed crystallographic information is given in Tables S5 and S6). The C5–N1 bond is found to be 1.288(3) Å, representing unsaturation (C=N) as compared to C13–N2 (saturated bond, C–N), with a bond length of 1.387(3) Å, confirming it to be a pyrazoline heterocycle. The C6–O1 bond length observed was 1.221 Å, depicting a C=O system. The bond length of the C=N system (C9–N3 and C20–N3) for the pyridyl ring was found to be 1.316(4) and 1.323(4) Å. The bond length for N1 and N2 was observed to be 1.387(3) Å (data pertaining to the X-ray diffraction studies of **PY1** can be



**SCHEME 1** Synthesis of *N*-pyridoyl- $\Delta^2$ -pyrazoline analogs (**PY1-PY13**)

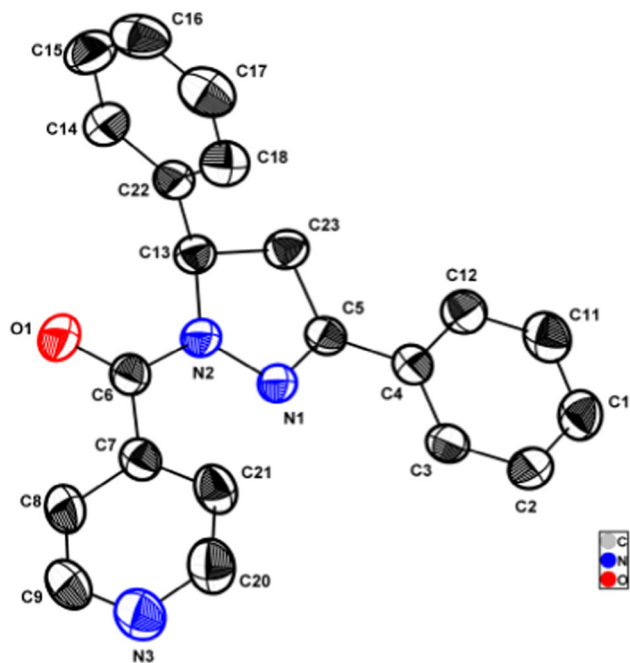


**FIGURE 3** Oak ridge thermal-ellipsoid plot program (ORTEP) diagram from X-ray crystallographic study of **PY1**

accessed through the Cambridge Crystallographic Data Center [CCDC] with the deposition number 1533986).

### 2.3 | In vitro cell proliferation assay

To evaluate the biological activity of the **PY** series, anti-proliferative activity screening by the 3-(4,5-dimethylthiazol-2-yl)-2,5-diphenyltetrazolium bromide (MTT) assay method was performed against human breast cancer cells MDA-MB-468 and human melanoma cells A375.<sup>[48]</sup> The activities of the *N*-pyridoyl- $\Delta^2$ -pyrazoline compounds (**PY1-PY13**) were compared with the reported Hsp90 inhibitor NVP-AUY922. **PY1-PY3** turned out to be the promising compounds among the series against breast and melanoma cancer cells (Table 1). The results suggest that **PY1-PY3** exhibited differential effects between cell lines of human breast cancer (MDA-MB-468) and human melanoma (A375). Compounds **PY1-PY3** exhibited a robust cytotoxic effect against human breast cancer with a range of  $IC_{50}$  values from 1.6 to 12  $\mu$ M. Compounds **PY1-PY3** were also found to have significant cytotoxic activity against human melanoma cells with a range of  $IC_{50}$  values from 7.7 to 22  $\mu$ M.

### 2.4 | Proteomic analysis

On the basis of the results of in vitro antiproliferative studies on human cancer cells, we carried out the proteomic analysis of hit compounds **PY1-PY3** to explore the Hsp90 protein interaction. Drug-affinity responsive target stability (DARTS), a recent proteomics approach to investigate small-molecule binding to targets using protease-based digestion, was performed on the cell lysates of human breast cancer

(MDA-MB-468).<sup>[49]</sup> The DARTS assay demonstrated that **PY1-PY3** protect Hsp90 $\beta$  from protease digestion similarly to RAD (see the 1/1,000 pronase dilution in Figures 4 and 5). The protection of Hsp90 against proteolysis is possible only because of the stable Hsp90-ligand complex formed by **PY** compounds. RAD also protects the Hsp90 protein against proteolysis. Untreated cell lysates failed to show the band of Hsp90, as the Hsp90 was proteolyzed by pronase to fragments. The in silico docking studies corroborate with the DARTS analysis, signifying that **PY1-PY3** interacts with Hsp90, and therefore shows promising antiproliferative activity.

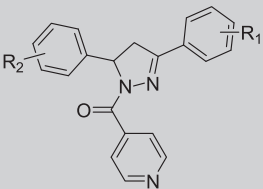
## 3 | CONCLUSION

In conclusion, the drug design, chemical synthesis, and biological evaluation of *N*-pyridoyl- $\Delta^2$ -pyrazolines are reported. The molecular modeling and docking simulations predicted the binding potential of the **PY** series in the N-terminal ATP-binding pocket of Hsp90. **PY** series have crucial polar interactions with the important residues of Hsp90, such as Asp93 and Thr184. In addition, nonpolar hydrophobic interactions were also responsible for the efficient binding of **PY1-PY3** with Hsp90, which is evident by an admirable docking score (-10.2 to -8.1 kcal/mol). Compounds **PY1** and **PY2** significantly reduced the human breast cancer cell proliferation ( $IC_{50}$  1.60 and 2.8  $\mu$ M), whereas **PY3** was moderate in action ( $IC_{50}$  12  $\mu$ M). Compound **PY1** was also found to be a promising inhibitor of human melanoma cells ( $IC_{50}$  7.7  $\mu$ M). Proteomic investigation in breast cancer cells implies the Hsp90 binding property of **PY1-PY3** molecules. All these investigations propose *N*-pyridoyl- $\Delta^2$ -pyrazolines (**PY1-PY3**) as promising anticancer compounds showing Hsp90 inhibition and show potential for further development as effective anticancer agents.

## 4 | EXPERIMENTAL

### 4.1 | Molecular modeling and docking simulations

Molecular docking simulations were carried out on the Dell workstation T1500 with the Windows 7 operating system using Schrodinger Maestro 9.1 drug design software.<sup>[43]</sup> The Hsp90 protein bound with GA (PDB ID: 1YET)<sup>[44]</sup> was downloaded from the RCSB Protein Data Bank for drug design studies. The protein was prepared by filling missing loops and missing side chains using a protein preparation wizard application of the Schrodinger software. Chain A of Hsp90 protein was further processed by removing nonreactive water molecules and crystal ligand (GA). The ionized protein having the lowest penalty was energy-minimized using the optimized potential for liquid simulations 2005 force field incorporated in the Impref tool of Glide programme to finally prepare processed 1YET protein. The grid was generated in the processed protein by excluding the docked ligand in the active site using a receptor grid generation tool of the Glide programme (the van der Waals radius-scaling factor was limited to 1.0 with a partial charge cut-off of 0.25). The active site was also predicted using DoGSiteScorer

**TABLE 1** Physical properties and anticancer activity of *N*-pyridoyl- $\Delta^2$ -pyrazoline analogs (PY1–PY13)


Compound	R <sub>1</sub>	R <sub>2</sub>	Yield (%)	m.p. (°C)	IC <sub>50</sub> (μM) ± SEM <sup>a</sup>	
					MDA-MB-468 <sup>b</sup>	A375 <sup>c</sup>
PY1	H	H	55	310	1.60 ± 0.06	7.73 ± 0.04
PY2	3',4'-OCH <sub>3</sub>	H	65	124	2.84 ± 0.05	15.45 ± 0.03
PY3	3',4'-OCH <sub>3</sub>	4''-OH, 3''-OCH <sub>3</sub>	73	157	12.05 ± 0.03	22.10 ± 0.48
PY4	2',4'-OCH <sub>3</sub>	4''-OCH <sub>2</sub> C <sub>6</sub> H <sub>5</sub> , 3''-OCH <sub>3</sub>	60	127	45.80 ± 0.06	47.25 ± 0.04
PY5	H	4''-OCH <sub>2</sub> C <sub>6</sub> H <sub>5</sub> , 3''-OCH <sub>3</sub>	65	147	45.10 ± 0.03	49.10 ± 0.12
PY6	3',4'-OCH <sub>3</sub>	3'',4''-OCH <sub>3</sub>	75	155	35.72 ± 0.03	48.87 ± 0.13
PY7	4'-Cl	3'',4''-OCH <sub>3</sub>	74	157	34.75 ± 0.15	40.32 ± 0.13
PY8	2',4'-OCH <sub>3</sub>	4''-OCH <sub>2</sub> C <sub>6</sub> H <sub>5</sub>	66	177	38.58 ± 0.16	35.87 ± 0.24
PY9	H	4''-OCH <sub>2</sub> C <sub>6</sub> H <sub>5</sub>	70	127	46.87 ± 0.23	43.57 ± 0.43
PY10	H	4''-Cl	75	150	48.68 ± 0.14	47.50 ± 0.18
PY11	2',4'-OCH <sub>3</sub>	4''-Cl	68	157	44.35 ± 0.34	48.57 ± 0.34
PY12	2',4'-OCH <sub>3</sub>	4''-OCH <sub>2</sub> C <sub>6</sub> H <sub>5</sub> (PF)	73	144	37.59 ± 0.43	47.59 ± 0.26
PY13	H	4''-OCH <sub>2</sub> C <sub>6</sub> H <sub>5</sub> (PF)	75	138	36.68 ± 0.37	38.98 ± 0.13
NVP-AUY922	-	-	-	-	0.012 ± 0.01	0.021 ± 0.03

Abbreviations: SEM, standard error of the mean; m.p., melting point.

<sup>a</sup>Data represent the IC<sub>50</sub> values for a 3-day exposure to normalized to no drug controls and is the mean of triplicate experiments performed; concentration ranges for PY1–PY3 compounds were 3.12 to 50 μM and for NVP-AUY922 12.5 to 200 nM.

<sup>b</sup>Human breast cancer.

<sup>c</sup>Human melanoma.

software.<sup>[41]</sup> The ligands were subjected to Ligprep simulations to generate energy-minimized three-dimensional structures (300 steps) by investigating tautomeric, stereochemical, and ionization variations. The ligprep out ligands were docked flexibly in the protein grid using Glide-extra precision (XP) simulations. Compounds having ≤300 atoms and

≤50 rotatable bonds were docked using five poses per ligand and 10,000 poses per docking run. Energies of residues within 12 Å of grid were used for simulations. Poses having coulomb–vdW energy greater than 0.0 kcal/mol and poses having an RMS deviation of 0.5 Å were discarded.<sup>[42]</sup> Finally, the docked ligands were scored based on the

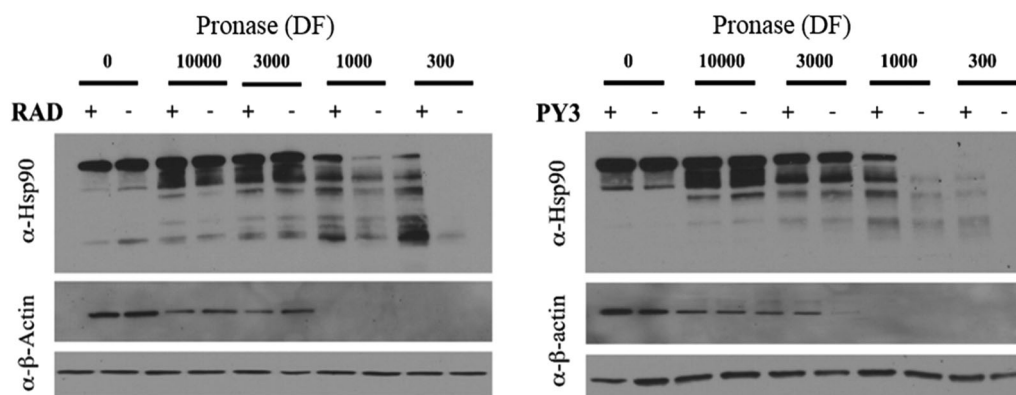


**FIGURE 4** Proteomic analysis of RAD and PY3 mediated protection of Hsp90 in MDA-MB-468 lysate. One millimolar RAD and PY3 protect Hsp90 from pronase degradation. Middle β-actin blot demonstrates the compound effect is specific for Hsp90 because of the equivalent proteolysis (+/-) compound. Bottom β-actin is a loading control from nonproteolyzed samples run simultaneously on a separate gel. Concentrations of pronase used are 1/10,000, 1/3,000, 1/1,000, and 1/300. DF, dilution factor; RAD, radicicol

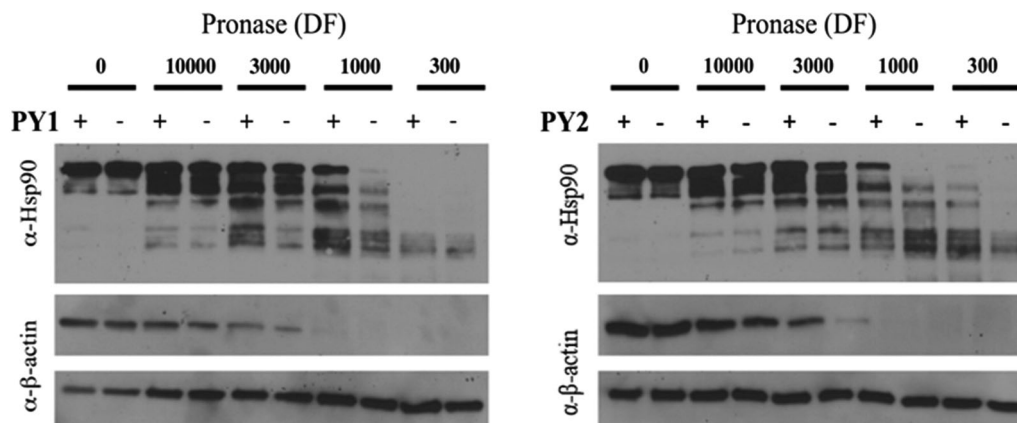


**FIGURE 5** Proteomic analysis of **PY1** and **PY2** analog mediated protection of Hsp90 in MDA-MB-468 cell lysate. One millimolar **PY1** and **PY2** protect Hsp90 from degradation. The specificity of this effect is indicated by equivalent  $\beta$ -actin degradation (+/-) compound (middle blot). The bottom  $\beta$ -actin blot acts as a loading control from the same sample but without proteolysis. Concentrations of pronase used are 1/10,000, 1/3,000, 1/1,000 and 1/300. DF, dilution factor

nonbonded interactions, such as lipophilic pair term, hydrogen bonding, hydrophobic enclosure reward, and electrostatic rewards.

Active site prediction for Hsp90, validation of docking methodology, extra precision (XP) docking results of Maestro 9.1 Glide, comparative docking interactions of the ligands in different crystal structures of Hsp90 protein, and crystallographic information of PY1 are provided as Supporting Information.

## 4.2 | Chemistry

$^1\text{H-NMR}$  spectra were recorded in  $\text{CDCl}_3$  on a Bruker Avance 300 MHz NMR spectrometer (Bruker BioSpin AG, Fallanden, Switzerland); chemical shifts ( $\delta$ ) were reported in ppm with tetramethylsilane as an internal standard. Mass fragmentation was recorded on an API2000 LC/MS mass spectrometer (Bruker Daltonics Inc., Billerica, MA). X-ray diffraction studies were done using Bruker-APEX III (X-ray diffractometer). Column chromatography was performed on Buchi flash chromatography with C-601 Pump Module, Pump Controller C-610, and Glass Column 26/230 cpl using silica gel (100–200 mesh). Infrared spectra were obtained from FT-IR-Affinity-1 spectrometer (Shimadzu, Japan). Uncorrected melting points were determined on an electrothermal melting point apparatus. Unless otherwise noted, all solvents and reagents were commercially available and used without further purification. The spectroscopic characterizations and original spectra of the synthesized compounds are provided in the Supporting Information.

## 4.3 | Biological activity

### 4.3.1 | Cell antiproliferative activity assay

The growth inhibitory activity of the test compounds was determined by MTT assay against human breast MDA-MB-468 and human melanoma A375 cells.<sup>[48]</sup> Each cell line was seeded on 96-well microplates at a

density of  $1.0 \times 10^4$  cells/well in 80  $\mu\text{l}$  and allowed to attach to the tissue culture-treated plastics after placing the 96-well plate in a Nuncoverplate for evaporation control for 4 hr. A five-step, two-fold drug dose dilution series was prepared robotically in a Biomek 3000 (Beckman Coulter) in the medium described previously. The test compounds were delivered as 20- $\mu\text{l}$  aliquots mixed into 80- $\mu\text{l}$  cell aliquot for a final exposure concentration. A Day-0 plate for each cell line was developed by the robotic addition of 10  $\mu\text{l}$  of 5 mg/ml MTT (in DMEM [Dulbecco's modified Eagle's medium], low glucose, 0% fetal bovine serum, and without phenol red) per well and allowed to develop for 4 hr after being placed in a Nuncoverplate to control evaporation. Then, 100  $\mu\text{l}$  of MTT solvent (0.1 N HCl in anhydrous isopropanol with 10% Triton X-100) was added, the assay plates were tightly wrapped in foil and placed in sealed zip lock bags to allow the solubilization of the MTT formazan product to occur and progress to solubilization for reading in a spectrophotometer at 570 nm. The subtraction of background absorbance measured at 690 nm was not performed. The Day-3 test plates were developed as described above.  $\text{IC}_{50}$  values were calculated using GraphPad Prism (Version 5.02, GraphPad software).

The InChI data of the PY series with anticancer activity against MDA MB468 and A375 cell lines are provided as Supporting Information.

### 4.3.2 | Hsp90-small-molecule inhibitor DARTs assay using whole-cell lysate<sup>[49]</sup>

MDA-MB-468 cells were lysed with lysis buffer (1 mM  $\text{NaVO}_3$ , 50 mM HEPES [4-(2-hydroxyethyl)-1-piperazineethanesulfonic acid], pH 7.4, 100 mM NaCl, 0.5% NP40, 1 mM EDTA [ethylenediaminetetraacetic acid], 1 mM EGTA [ethylene glycol-bis( $\beta$ -aminoethyl ether)- $N,N,N',N'$ -tetraacetic acid], 50  $\mu\text{g}/\text{ml}$  RNase, 1% Triton X-100, 1% deoxycholic acid, 1  $\mu\text{g}/1 \mu\text{l}$  leupeptin or Roche protease inhibitor mixture and  $1\times$  protease mixture) for 15 min at 25°C. After centrifugation (13,200 rpm using Eppendorf microcentrifuge 5415D; 15 min), the protein concentration of the lysate was measured using MicroBCA™ protein assay kit. Twenty-five

micrograms of protein cell lysate was incubated with 1 mM compound and binding buffer (50 mM Tris HCl pH 8.0, 50 mM NaCl, 10 mM CaCl<sub>2</sub>) to a 20- $\mu$ l final volume for 2 hr at room temperature. Samples were digested with Pronase (Roche) at varying dilutions for 15 min at 25°C. The reaction was stopped by the addition of 5  $\mu$ l of 5 $\times$  sodium dodecyl sulfate (SDS) loading dye and this was immediately followed by boiling samples at 95°C for 5 min. Samples were run in 4–15% gradient SDS-PAGE (SDS-polyacrylamide gel electrophoresis) gels at 150 V for 60 min followed by Western blot analysis. An equal aliquot of the nonproteolyzed sample was run simultaneously on a separate gel to assess  $\beta$ -actin levels as a loading control. Blots were probed with anti-Hsp90 antibody (ADI-SPA-831; Enzo Life Sciences). The blots were stripped and reprobed with anti- $\beta$ -actin antibody (JLA20; DSHB University of Iowa) to demonstrate that the  $\beta$ -actin was proteolyzed equally in the presence or absence of compound, and hence the compound-mediated protection of Hsp90 was specific. The same anti- $\beta$ -actin antibody was used to probe  $\beta$ -actin levels in the loading control gel.

## ACKNOWLEDGMENTS

We are thankful to the Department of Health Research (V.25011/283/2014-HR), Ministry of Health & Family Welfare, Government of India, and the Rajiv Gandhi University of Health Sciences, Karnataka (Advanced Research Project 2019–2020), India, for providing financial and moral assistance to this project. We thank Dr. Vincent Jo Davisson, Dr. Tony Hazbun, and Mr. Raymond Fatig of the MCMP Department, Purdue University, USA, for their constructive suggestions and support throughout the project.

## CONFLICT OF INTERESTS

The authors declare that there are no conflict of interests.

## ORCID

Nulgumnalli Manjunathaiah Raghavendra  <http://orcid.org/0000-0002-0846-012X>

## REFERENCES

- [1] L. H. Pearl, C. Prodromou, *Annu. Rev. Biochem.* **2006**, *75*, 271.
- [2] D. Hanahan, R. A. Weinberg, *Cell* **2000**, *100*, 57.
- [3] L. Neckers, P. Workman, *Clin. Cancer Res.* **2012**, *18*, 64.
- [4] B. S. J. Blagg, T. D. Kerr, *Med. Res. Rev.* **2005**, *26*, 310.
- [5] A. Maloney, P. Workman, *Expert Opin. Biol. Ther.* **2002**, *2*, 3.
- [6] P. Workman, *Curr. Cancer Drug Targets* **2003**, *3*, 297.
- [7] B. K. Eustace, T. Sakurai, J. K. Stewart, D. Yimlamai, C. Unger, C. Zehetmeier, B. Lain, C. Torella, S. W. Henning, G. Beste, B. T. Scroggins, L. Neckers, L. L. Ilag, D. G. Jay, *Nat. Cell Biol.* **2004**, *6*, 507.
- [8] Q. Cheng, J. T. Chang, J. Geradts, L. M. Neckers, T. Haystead, N. L. Spector, H. K. Lysterly, *Breast Cancer Res.* **2012**, *14*, R62.
- [9] L. Whitesell, E. G. Mimnaugh, B. de Costa, C. E. Myers, L. M. Neckers, *Proc. Natl. Acad. Sci. USA* **1994**, *91*, 8324.
- [10] J. G. Supko, R. L. Hickman, M. R. Grever, L. Malspeis, *Cancer Chemother. Pharmacol.* **1995**, *36*, 305.
- [11] R. C. Schnur, M. L. Corman, R. J. Gallaschun, B. A. Cooper, M. F. Dee, J. L. Doty, M. L. Muzzi, J. D. Moyer, C. I. DiOrio, E. G. Barbacci, P. E. Miller, A. T. O'Brien, M. J. Morin, B. A. Foster, V. A. Pollack, D. Savage, D. E. Sloan, L. R. Pustilnik, M. P. Moyer, *J. Med. Chem.* **1995**, *38*, 3806.
- [12] E. Sausville, J. Tomaszewski, P. Ivy, *Curr. Cancer Drug Targets* **2003**, *3*, 377.
- [13] J. L. Eisman, J. Lan, T. F. Lagattuta, D. R. Hamburger, E. Joseph, J. M. Covey, M. J. Egorin, *Cancer Chemother. Pharmacol.* **2005**, *55*, 21.
- [14] S. Tanida, T. Hasegawa, E. Higashide, *J. Antibiot.* **1980**, *33*, 199.
- [15] K. Shibata, S. Satsumabayashi, A. Nakagawa, S. Omura, *J. Antibiot.* **1986**, *39*, 1630.
- [16] N. Winssinger, S. Barluenga, *Chem. Commun. (Camb)* **2007**, *1*, 22.
- [17] G. E. L. Brandt, M. D. Schmidt, T. E. Prisinzano, B. S. J. Blagg, *J. Med. Chem.* **2008**, *51*, 6495.
- [18] P. V. Borges, K. H. Moret, N. M. Raghavendra, T. E. Maramaldo Costa, A. P. Monteiro, A. B. Carneiro, P. Pacheco, J. R. Temerozo, D. C. Bou-Habib, M. das Graças Henriques, C. Penido, *Pharmacol. Res.* **2017**, *115*, 65.
- [19] G. Chiosis, M. N. Timaul, B. Lucas, P. N. Munster, F. F. Zheng, L. Sepp-Lorenzino, N. Rosen, *Chem. Biol.* **2001**, *8*, 289.
- [20] M. G. Rowlands, Y. M. Newbatt, C. Prodromou, L. H. Pearl, P. Workman, W. Aherne, *Anal. Biochem.* **2004**, *327*, 176.
- [21] P. A. Brough, W. Aherne, X. Barril, J. Borgognoni, K. Boxall, J. E. Cansfield, K. M. J. Cheung, I. Collins, N. G. M. Davies, M. J. Drysdale, B. Dymock, S. A. Eccles, H. Finch, A. Fink, A. Hayes, R. Howes, R. E. Hubbard, K. James, A. M. Jordan, A. Lockie, V. Martins, A. Massey, T. P. Matthews, E. McDonald, C. J. Northfield, L. H. Pearl, C. Prodromou, S. Ray, F. I. Raynaud, S. D. Roughley, S. Y. Sharp, A. Surgenor, D. L. Walmsley, P. Webb, M. Wood, P. Workman, L. Wright, *J. Med. Chem.* **2008**, *51*, 196.
- [22] E. McDonald, K. Jones, P. Brough, M. Drysdale, P. Workman, *Curr. Top. Med. Chem.* **2006**, *6*, 1193.
- [23] T. Y. Lin, M. Bear, Z. Du, K. P. Foley, W. Ying, J. Barsoum, C. London, *Exp. Hematol.* **2008**, *36*, 1266.
- [24] A. J. Woodhead, H. Angove, M. G. Carr, G. Chessari, M. Congreve, J. E. Coyle, J. Cosme, B. Graham, P. J. Day, R. Downham, L. Fazal, R. Feltell, E. Figueroa, M. Frederickson, J. Lewis, R. McMenamin, C. W. Murray, M. A. O'Brien, L. Parra, S. Patel, T. Phillips, D. C. Rees, S. Rich, D. M. Smith, G. Trewartha, M. Vinkovic, B. Williams, A. J. A. Woolford, *J. Med. Chem.* **2010**, *53*, 5956.
- [25] R. Bao, C. J. Lai, H. Qu, D. Wang, L. Yin, B. Zifcak, R. Atoyian, J. Wang, M. Samson, J. Forrester, S. Della Rocca, G. X. Xu, X. Tao, H. X. Zhai, X. Cai, C. Qian, *Cancer Res.* **2009**, *15*, 4046.
- [26] K. H. Huang, J. M. Veal, R. P. Fadden, J. W. Rice, J. Eaves, J. P. Strachan, A. F. Barabasz, B. E. Foley, T. E. Barta, W. Ma, M. A. Silinski, M. Hu, J. M. Partridge, A. Scott, L. G. DuBois, T. Freed, P. M. Steed, A. J. Ommen, E. D. Smith, P. F. Hughes, A. R. Woodward, G. J. Hanson, W. S. McCall, C. J. Markworth, L. Hinkley, M. Jenks, L. Geng, M. Lewis, J. Otto, B. Pronk, K. Verleysen, S. E. Hall, *J. Med. Chem.* **2009**, *52*, 4288.
- [27] J. C. Bendell, T. M. Bauer, R. Lamar, M. Joseph, W. Penley, D. S. Thompson, D. R. Spigel, R. Owerka, C. M. Lane, C. Earwood, H. A. Burris, *Cancer Invest.* **2016**, *34*, 265.
- [28] W. Ying, Z. Du, L. Sun, K. P. Foley, D. A. Proia, R. K. Blackman, D. Zhou, T. Inoue, N. Tatsuta, J. Sang, S. Ye, J. Acquaviva, L. S. Ogawa, Y. Wada, J. Barsoum, K. Koya, *Mol. Cancer Ther.* **2012**, *11*, 475.
- [29] W. Xu, L. Neckers, *Clin. Cancer Res.* **2007**, *13*, 1625.
- [30] R. M. Immormino, Y. Kang, G. Chiosis, D. T. Gewirth, *J. Med. Chem.* **2006**, *49*, 4953.
- [31] P. Fadden, K. H. Huang, J. M. Veal, P. M. Steed, A. F. Barabasz, B. Foley, M. Hu, J. M. Partridge, J. Rice, A. Scott, L. G. Dubois,

- T. A. Freed, M. A. R. Silinski, T. E. Barta, P. F. Hughes, A. Ommen, W. Ma, E. D. Smith, A. W. Spangenberg, J. Eaves, G. J. Hanson, L. Hinkley, M. Jenks, M. Lewis, J. Otto, G. J. Pronk, K. Verleysen, T. A. Haystead, S. E. Hall, *Chem. Biol.* **2010**, *17*, 686.
- [32] T. Force, D. S. Krause, R. A. van Etten, *Nat. Rev. Cancer* **2007**, *7*, 332.
- [33] B. B. Hasinoff, D. Patel, K. A. O'Hara, *Mol. Pharmacol.* **2008**, *74*, 1722.
- [34] C. Prodromou, L. Pearl, *Curr. Cancer Drug Targets* **2003**, *3*, 301.
- [35] S. Dutta Gupta, M. K. Bommakka, G. I. Mazaira, M. D. Galigniana, C. V. S. Subrahmanyam, N. L. Gowrishankar, N. M. Raghavendra, *Int. J. Biol. Macromol.* **2015**, *80*, 253.
- [36] S. Dutta Gupta, B. Revathi, G. I. Mazaira, M. D. Galigniana, C. V. S. Subrahmanyam, N. L. Gowrishankar, N. M. Raghavendra, *Bioorg. Chem.* **2015**, *59*, 97.
- [37] S. Dutta Gupta, D. Snigdha, G. I. Mazaira, M. D. Galigniana, C. V. S. Subrahmanyam, N. L. Gowrishankar, N. M. Raghavendra, *Biomed. Pharmacother.* **2014**, *68*, 369.
- [38] S. Kadasi, T. E. M. M. Costa, N. Arukala, M. Toshakani, C. Dugginetti, S. Thota, S. D. Gupta, S. Raj, C. Penido, M. G. Henriques, N. M. Raghavendra, *Med. Chem.* **2018**, *14*, 44.
- [39] P. A. Brough, X. Barril, M. Beswick, B. W. Dymock, M. J. Drysdale, L. Wright, K. Grant, A. Massey, A. Surgenor, P. Workman, *Bioorg. Med. Chem. Lett.* **2005**, *15*, 5197.
- [40] Y. Yang, H. Liu, J. Du, J. Qin, X. Yao, *J. Mol. Model.* **2011**, *17*, 3241.
- [41] A. Volkamer, D. Kuhn, F. Rippmann, M. Rarey, *Bioinformatics* **2012**, *28*, 2074.
- [42] K. E. Hevener, W. Zhao, D. M. Ball, K. Babaoglu, J. Qi, S. W. White, R. E. Lee, *J. Chem. Inf. Model.* **2009**, *49*, 444.
- [43] *Maestro 9.1*, Schrödinger, LLC, New York, NY; **2011**.
- [44] C. E. Stebbins, A. A. Russo, C. Schneider, N. Rosen, F. U. Hartl, N. P. Pavletich, *Cell* **1997**, *89*, 239.
- [45] W. M. J. Obermann, H. Sondermann, A. A. Russo, N. P. Pavletich, F. U. Hartl, *J. Cell Biol.* **1998**, *143*, 901.
- [46] J. M. Jez, J. C. H. Chen, G. Rastelli, R. M. Stroud, D. V. Santi, *Chem. Biol.* **2003**, *10*, 361.
- [47] C. Austin, S. N. Pettit, S. K. Magnolo, J. Sanvoisin, W. Chen, S. P. Wood, L. D. Freeman, R. J. Pengelly, D. E. Hughes, *J. Biomol. Screen.* **2012**, *17*, 868.
- [48] M. V. Berridge, P. M. Herst, A. S. Tan, *Biotechnol. Annu. Rev.* **2005**, *11*, 127.
- [49] B. Lomenick, R. Hao, N. Jonai, R. M. Chin, M. Aghajan, S. Warburton, J. Wang, R. P. Wu, F. Gomez, J. A. Loo, J. A. Wohlschlegel, T. M. Vondriska, J. Pelletier, H. R. Herschman, J. Clardy, C. F. Clarke, J. Huang, *Proc. Natl. Acad. Sci. USA* **2009**, *106*, 21984.

## SUPPORTING INFORMATION

Additional supporting information may be found online in the Supporting Information section.

**How to cite this article:** Kadasi S, Yerroju R, Gaddam S, et al. Discovery of *N*-pyridoyl- $\Delta^2$ -pyrazolines as Hsp90 inhibitors. *Arch Pharm Chem Life Sci.* 2019;e1900192. <https://doi.org/10.1002/ardp.201900192>